Title: Geometrical Shape Influence on Energy Harvesting Performance of Oscillating Airfoil

Sarah A'fifah Abdullah Sani
Computational Engineering Design Group, Faculty of Engineering & Environment, University of Southampton, Southampton, UK.
saas1y12@soton.ac.uk

Kamal Djidjeli
Computational Engineering Design Group, Faculty of Engineering & Environment, University of Southampton, Southampton, UK.
kkd@soton.ac.uk

Jing Tang Xing
Fluid Structure Interaction Group, Faculty of Engineering & Environment, University of Southampton, Southampton, UK.
jtxing@soton.ac.uk

Paper submission to Sustainable Development Conference 2016

Abstract:
In recent years, as an alternative to conventional turbomachinery, flapping foils or oscillating airfoils are under increasingly active investigation to extract energy from wind/water. Their potentials for the generation of electric power are studied here computationally using a two-dimensional unsteady Navier-Stokes solver. In this study, the effect of geometrical shape variation on energy harvesting performance of oscillating airfoil have been investigated. A selective range of parameters have been investigated for symmetrical airfoils (NACA0012, NACA0015, and NACA0018), including the airfoil geometrical parameters: thickness distribution and trailing edge shapes (sharp, blunt and round); fundamental kinematics parameters, i.e. frequency oscillation ($f^* = 0.10 - 0.20$) at fixed heaving and pitching amplitudes, and the effect of fluid physics (laminar flow at *Re* = 1100 and turbulent flow at *Re* = $5x10^5$) are considered. For the turbulent simulations, the highly resolve numerical simulations ($y^+ \leq 1$) are performed at high pitch angles using the $k - \omega$ SST turbulence model, which is found to model the flow separation effectively. The power-extraction efficiency has been used as the performance comparison metric to map the performance into the parametric space considered in this study. The peak efficiency for laminar case has occurred at frequency, $f^* = 0.14$ meanwhile for turbulent case, high efficiency has occurred at frequency, $f^* = 0.18$ and $\theta_0 = 76.3°$. Less than 2% differences in power efficiency has been observed on the study of the effect of thickness distribution at low Reynolds number, while about 10 to 16% difference has been found for high Reynolds number by comparing NACA0018 and NACA0012 airfoils. Both laminar and turbulent flows show that sharp edge gives the most optimum efficiency performance, with the highest efficiency for laminar is 33.3% while for turbulent is 44.5%.

Keywords – oscillating airfoil; energy harvesting; laminar and turbulent flow field.

Introduction

Fossil fuel continue to be the major energy resource to the world as compared to renewable resources, (contributing approximately 70%) [1]. However, these resources are known to be of limited stock and the environmental impact of these resources motivate the researchers to develop alternative renewable resources such as; wind, hydro and solar. Hydro resources are the most predictable and economically feasible renewable resource [2]. At present conventional tidal turbomachinery requires a techno-economic flow speed around 2.5 – 3.2 m/s [3], whereby as indicated by [4] technically feasible potential of tidal resource can be twice by lower the operating flow speed to 1.8 m/s.

The mechanical vibration energy resources are based on the flow induced vibration and fluid-structure interaction. One of the technologies that merging this concept is flapping foils or oscillating airfoil system, as they generate spontaneous, self-sustained and large amplitudes vibration that can be couple with the electrical generators to produce electricity [5]. This technology is capable of extracting energy at extremely low airfoil velocities (less than 1 m/s) as compared to rotary turbomachinery. The unique advantages of oscillating airfoils also includes shallow water operation, lower environmental and wildlife impact, small scale power generation and low noise emission [6].

The concept of oscillating airfoils was initially proposed by McKinney and Delaurier [7] in 1981 where they have performed analytical and experimental analyses of flow over a flapping-wing power generator in order to examine its feasibilities. Under applied fluid kinematics parameters of pitch angle of 30° and angle of attack of 15^{o}, McKinney and Delaurier have reported a power efficiency of 17%. Moreover, they showed that unsteady aerodynamics achieve high power efficiency as compared to linear analytical analysis [7]. Later, Kinsey and Dumas [8] carried out computational study to parametrize the influence of fluid kinematic variables on the energy harvesting characteristics of oscillating airfoil systems. The key contribution of his work includes optimization of pitch and heaving amplitudes of oscillating airfoils at particular oscillating frequencies. It was reported that a higher value of power efficiency around 34% can be extracted from the oscillating airfoil at comparatively higher pitch angle of 76.33°. They have also concluded that, leading edge vortices (LEVs) is one of the key parameters to enhanced power generation in flapping airfoil system at low Reynolds number. John Young et. al [9] have also computationally analysed the performance of flow driven flapping wing turbines for wind and water power generation at low Re values of 1100 for prescribed-motion. The research achieved a higher power efficiency value of 30%. At present, the research activities in the fields of oscillating energy harvesting system mainly focused on exploring the highest feasible power generation at low speed and small scale as cited in nature [10] and also to reproduce similar effect in turbulent flow regimes to develop large scale real world applications.

It can be concluded that significant focus is directed towards the investigation of fundamental parameters and the influence on the energy harvesting characteristic of oscillating airfoil such as heaving and pitching amplitude, frequency, phase angle, oscillating motion etc. [11]–[13]. However, the effect of geometry to the power performance is rarely been studied. Therefore, current work comprises the study of the flapping foil geometrical features that includes the effect of thickness distribution, trailing edge shape modification, and a range of frequencies. The numerical simulations in this study are performed with an Eulerian approach and conformal sliding mesh strategy, using the commercial code Ansys Fluent software.

Motion Description

The oscillating airfoil motion in this study has been implemented as combined pitch and heave airfoil motion. Figure 1 shows the imposed heaving and pitching motion at phase angle, $\phi = 90°$.

For an oscillating airfoil operating in free stream velocity U_∞, as shown in Figure 2, the combined pitch-heave motion is mathematically expressed as sinusoidal functions [8]:

$$\theta(t) = \theta_0 \sin(\omega t) \quad (1)$$

$$h(t) = H_0 \sin(\omega t + \phi) \quad (2)$$

where H_0 and θ_0 are respectively, the heaving and pitching amplitudes. ω is the angular frequency ($\omega = 2\pi f$), f is the oscillating frequency and ϕ is the phase angle between the pitching and heave motion.

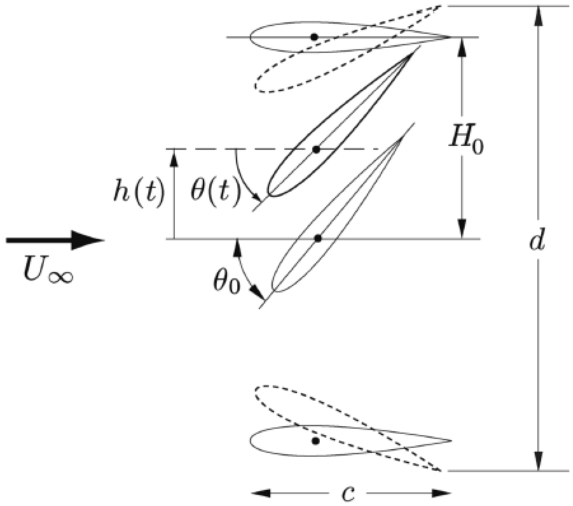

Figure 1: Imposed pitching and heaving motion ($\phi = 90^\circ$) [8]

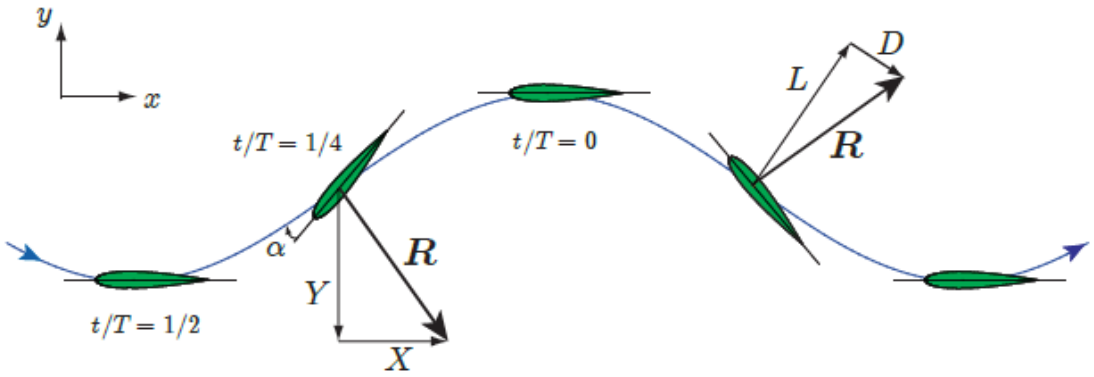

Figure 2: An oscillating airfoil illustrated in a freestream velocity reference frame [8]

Figure 2 shows the resultant aerodynamic force on an airfoil has a vertical component which is in the same direction as the vertical displacement; therefore, the flow performs positive work and power is extracted from the flow because no negative work is involved with respect to horizontal component.

Extracted Power and Efficiency

To quantify the value of extracted power, the time-averaged method is used, where it defines as integrating the instantaneous power extracted in one cycle. The instantaneous power extracted from

the flow comes from the sum of a heaving contribution, $P_y(t) = Y(t)dh/dt$ and a pitching contribution, $P_\theta(t) = M(t)d\theta/dt$, where $Y(t)$ is vertical component of aerodynamic force; $M(t)$ is the torque about the pitching axis, x_p. The instance power extraction and the time-averaged extracted power can be expressed as [8]:

$$P(t) = Y(t)\, dh/dt + M(t)\, d\theta/dt \tag{3}$$

$$\acute{P} = 1/T \int_t^{t+T} P\, dt \tag{4}$$

The power coefficient, C_P is defines as the ratio of extracted power P to the total of available power in the free stream. Hence, the mean power coefficient in one cycle can be expressed as [8]:

$$\bar{C_p} = \acute{P}/(0.5\rho U_\infty{}^3 c) \tag{5}$$

Meanwhile, the power extraction efficiency, η is represented as the ratio of the total extracted power to the total incoming flow energy flux within the swept area [8]:

$$\eta = \bar{C_p}\ (c/d) \tag{6}$$

where c and d are the airfoil chord length and the total vertical distance swept by the airfoil leading or trailing edge.

Numerical Methodology

A. Computational Modelling

In all cases presented in this study, the problem is set in a heaving reference frame (vertical translation) attached to the airfoil. The pitching motion of the airfoil motion is rotating in the translating reference frame. This implies the use of time-varying velocity conditions on the inflow domain boundary and the addition of a new source term in the Navier-Stokes equation to account for the reference-frame acceleration. Hence, mesh motion is necessary only for rotating (pitching) motion of the airfoil. This is done by splitting the domain into different zones bounded by a circular conformal sliding interface. The motion of the airfoil is prescribed in ANSYS Fluent V.14.5 through the use of user-defined functions (UDFs) compiled within the solver. The 2D unsteady Navier-Stokes solver flow simulation in this study was modelled as incompressible flow, and the performance behaviour of flapping foils is analyzed for laminar and turbulent flow characteristics.

For laminar flow fields, a second order accurate upwind scheme is used to discretize convection term, and diffusion-term discretization is done with the second-order central-differencing schemes. A second-order backward implicit scheme is used to discretize time. Semi-implicit method for pressure-linked algorithm SIMPLE is used for the velocity-pressure coupling. Gauss-Seidel linear equation solver is used for the discretized equations.

For turbulent flow fields, the turbulence modelling of two-equations $k-\omega$ SST (low-Re correction) has been chosen. Again the SIMPLE algorithm has been selected for pressure-velocity coupling. Second order schemes are used for pressure, momentum and turbulent viscosity resolution. The unsteady formulation is based on a second order implicit scheme and absolute convergence criteria of 10^{-5} are set for continuity and velocity components while 10^{-4} is used for the turbulent viscosity.

B. Geometrical Modelling

Pointwise commercial mesh software [14] has been used to model the simulation domain and IGES file is the compatible geometrical format required by this package. For this particular requirement, the

coordinate data points of NACA profiles has been imported in the SolidWorks CAD modeler. As per scope of the present study, the required geometrical modifications of the trailing edge shape, i.e. sharp, blunt and round edges have been carried out in the SolidWorks environment and then exported the IGES file format into pointwise meshing tool. Three different symmetrical airfoils have been used in this study which are NACA0012, NACA0015 and NACA0018 (Figure 3). All of these airfoils have undergone the same procedure for trailing edge modifications, as shown in Figure 4.

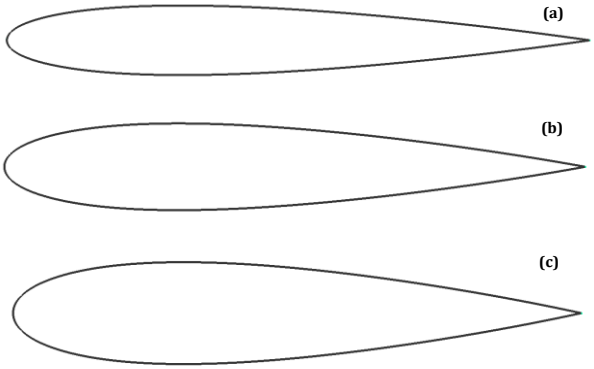

Figure 3: Three different airfoils (a) NACA0012 (b) NACA0015 (c) NACA0018

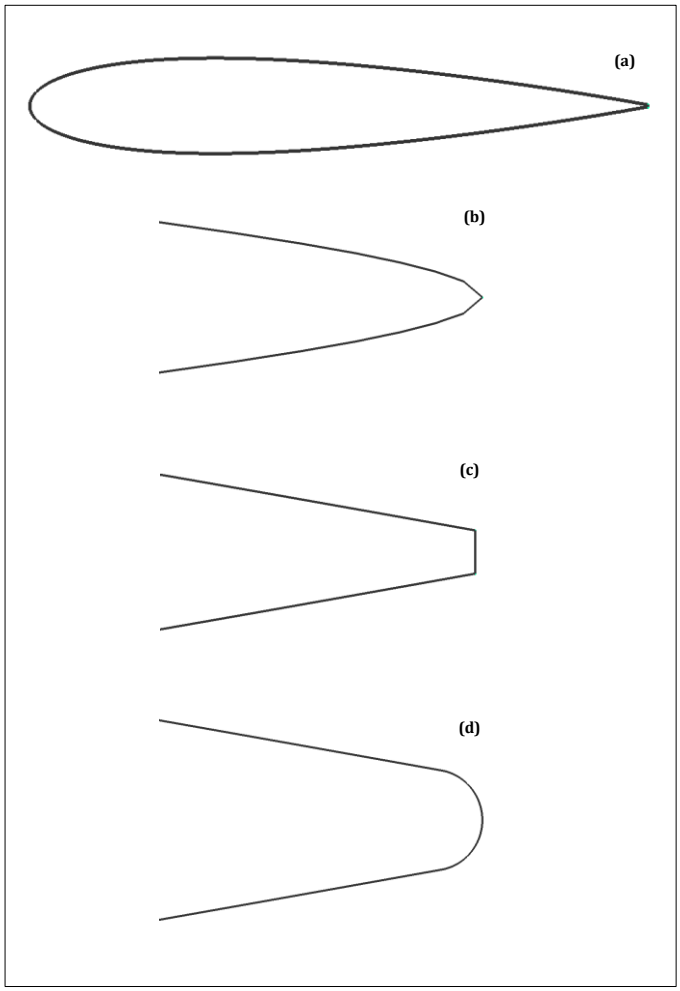

Figure 4: (a) NACA0015 with different trailing edge shapes (b) close-up view of sharp edge (c) close-up view of blunt edge (d) close-up view of round edge

All cases have been simulated using structured grid. The structured grid was developed using O-H topology, as shown in Figure 5(a). The close-up near wall is displayed in Figure 5(c). In this work,

a sufficiently large computational domain with reference to the flapping foil chord length '*c*' is used in all of the simulation cases to avoid reverse flow. The upstream inlet velocity boundary and the downstream pressure outlet were located at 35*c* and 40*c* from the pitching point, respectively. The upper and lower flow boundaries were placed at 35*c* from the pitching point.

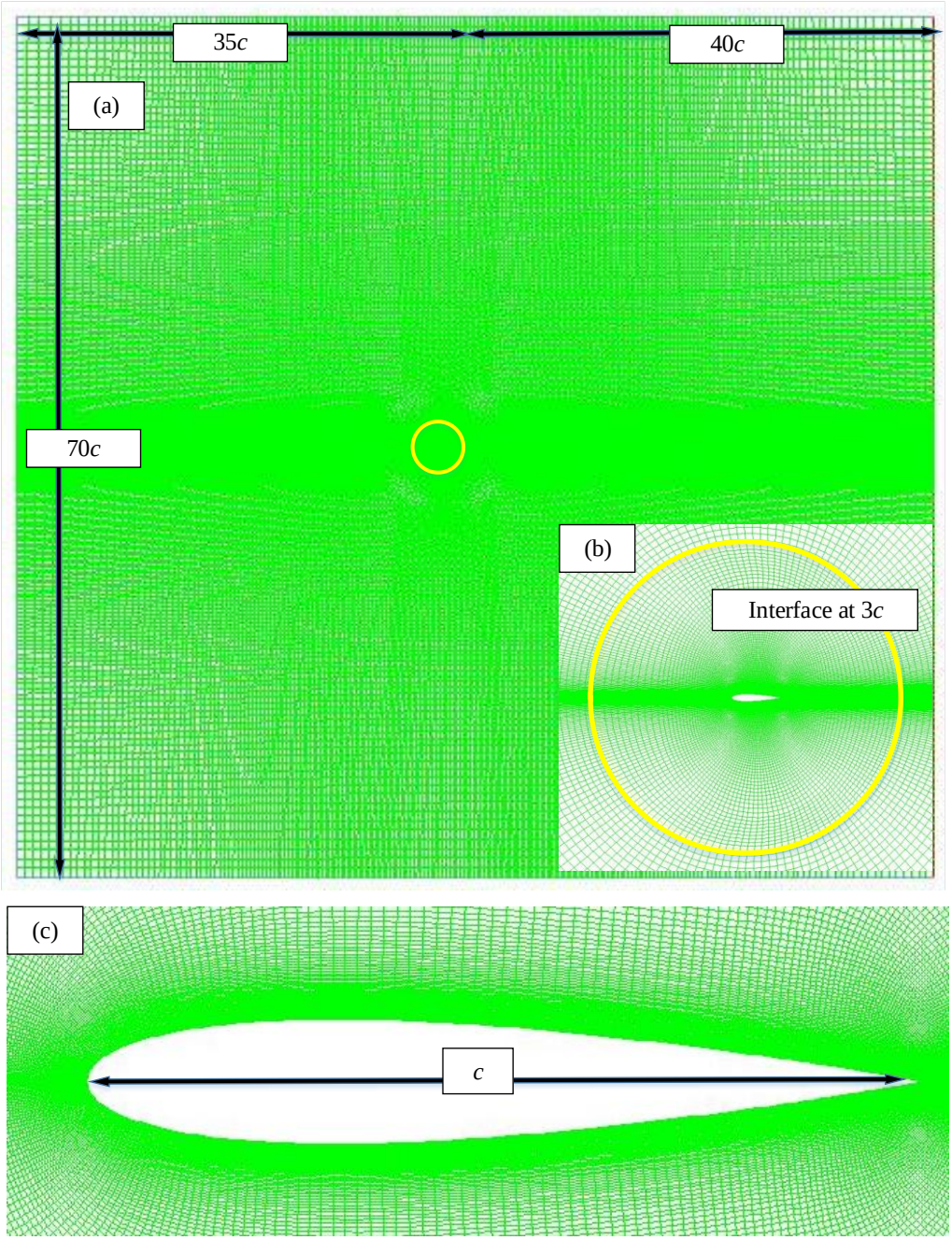

Figure 5: (a) Simulation domain, (b) location of interface, (c) close-up view near wall of the Naca0015

Numerical Validation

Fluid structure interaction study of oscillating airfoils is complex in nature due to aerodynamic behaviour of moving airfoils and resulting large flow separation over the periodic cycle of oscillation. At present there is no experimental data available to validate the implemented design space of geometrical variation of foil system used in this study. CFD based numerical predictions are approximate solutions that require sufficiently refine mesh resolution as a fundamental requirement

such that the discretization error is not only small in magnitude but also shows an asymptotic behaviour [18]. In order to have reliable flow parameter predictions, a rigorous 2D mesh sensitivity analysis together with numerical validations of similar airfoil geometry under identical case setup of [8], [15] has been done for laminar and turbulent flow regimes. Due time and computational resource constraints, it is not feasible to numerically resolve all the instances of parametric design space of geometric and fluid flow parameters. Therefore to carry out this two-step validation process a base line NACA 0015 sharp trailing edge airfoil system is selected.

First of all to optimize the discretization error for both space and time a set of three structured grids are generated following the procedure outlined in the above section (Grid generation) in an order of increasing mesh densities for airfoil surface, rotational and stationery fluid zones. For coarse, medium, and refine mesh the number of computational nodes on the airfoil surface are 150, 300, 500, respectively. The corresponding total cells count of 2D cross sections of simulated domain are shown in Table 1. The simulations are run for sufficiently large number of cycles before the targeted residual values of 10^{-5} for pressure, velocity and turbulence parameters has been achieved. Statistically averaged values of aerodynamic performance coefficients of oscillating airfoil systems, i.e. C_l and C_Y from converged solution have been setup to estimate the mesh resolution and numerical discretization errors. The case setup involves NACA0015 undergoing sinusoidal pitching and heaving motion at Reynolds number of 1100 in order to examine the power extraction performance with parameters setup of $H_0 = 1$, θ_0=76.3°, and $f^* = 0.14$, where the dimensionless frequency is defined as $f^* = fc/U_\infty$. These parameters values were chosen, as they are found to have an optimum performance by Kinsey and Dumas [8].

MESH RESOLUTION	CELLS
Coarse	58,479
Medium	155,010
Refine	300,027

Table 1: Description of mesh sensitivity analysis

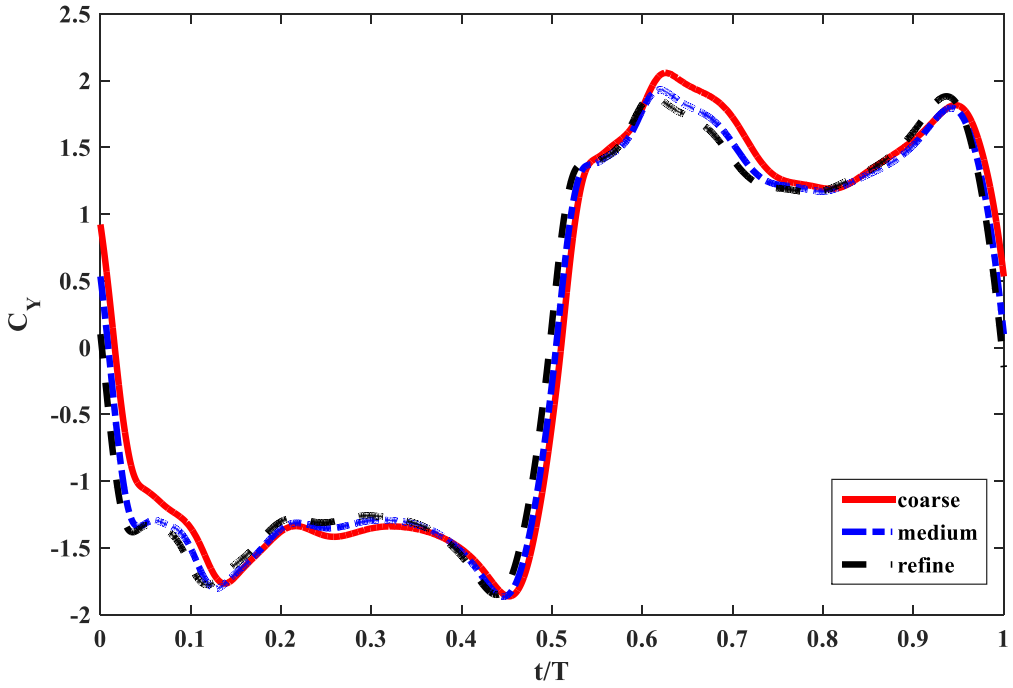

Figure 6: Comparison of performance for coarse, medium and fine mesh

Figure 6 shows the comparison of performance between the coarse, medium and fine mesh. As can be seen, the medium and fine meshes give much closer results. For numerical validation, with the previous published work [8], [15], the medium mesh resolution is selected. Table 2 shows the results for the efficiency, η and power coefficient, $\bar{C}_P$ of the flapping NACA0015 airfoil at *Re* = 1100, with the corresponding results of Kinsey and Dumas [8]. The results in Table 2 show that our results (present study) compare well with those of Kinsey and Dumas [8]; and the overall differences are less than 5%.

STUDY	EFFICIENCY , η	POWER COEFFICIENT, $\bar{C}_P$
Present	33.3%	0.85
Kinsey & Dumas [8]	33.7%	0.86

Table 2: Parametric study of flows over flapping NACA0015 airfoil at *Re* = 1100

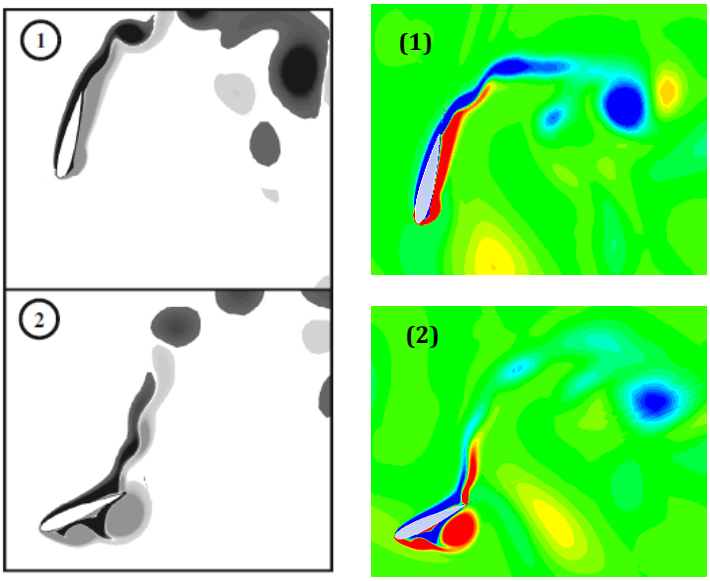

Figure 7: Comparison of vorticity contour of Kinsey and Dumas work (left) and present study (right), (1) at 0.25T, and (2) at 0.45T

Figure 7 shows the vorticity contours of Kinsey and Dumas [8] and the current study (right figures) at 0.25T and 0.45T. These results show similar trends.

In order to further perform the convergence validation, the simulation of imposed pitching-heaving motion of NACA0015 has also been carried out in turbulence flow field at $Re = 5 \times 10^5$, $f* = 0.14$, $\theta_0 = 76.3°$. The turbulence model used is the $k - \omega$ SST with low-Re correction. The turbulent inlet boundary condition for this model has been characterized as an intensity of 0.1% and a turbulent viscosity ratio of 0.01. These stated parameters have been chosen in order to validate the current results with the published work by Kinsey and Dumas [15]. The results were presented in Table 3 and Figure 8.

STUDY	EFFICIENCY , η	POWER COEFFICIENT, $\overline{C}_P$
Present	39.34%	1.0032
Kinsey & Dumas [15]	39.94%	1.018

Table 3: Parametric study of flows over a flapping NACA0015 airfoil at $Re = 5 \times 105$, $f* = 0.14$, $H_0 = 1$, $x_p = 1/3$

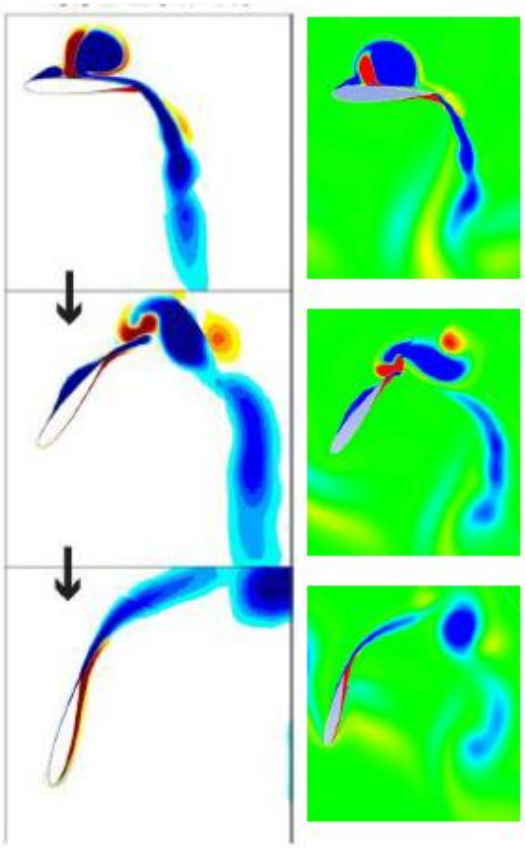

Figure 8: Comparison of vorticity contour of Kinsey and Dumas work (left) and present study (right) at t/T=0, 0.125, and 0.25T

Again, good agreement is achieved in this case. Therefore it can be concluded that the opted numerical methodology is a suitable numerical method for the current investigations.

Results

In this section, numerical findings of the foil system geometrical variation has been discussed. The present data parametrically map the variation in thickness distribution and trailing edge shape. The results for each geometry modification has been compiled distinctly for laminar *Re* = 1100 and turbulent flow (*Re* = 5 x 10^5) while power efficiency of simulated results is compared to explore optimum design configuration. Fluid kinematics parameters such as oscillating frequencies (f^* = 0.10 – 0.20), pitching amplitude, $\theta_0 = 76.3°$ and heaving amplitudes $H_0 = 1$ are held constant for the simulated cases to explicitly identify the effect of geometrical parameters in applied fluid physics regimes.

A. Effect of Thickness Distribution on Performance Efficiency

Thickness distribution is one of the varied parameter in this study. Here, three different NACA airfoils, mainly NACA0012, NACA0015 and NACA0018, have been chosen in order to investigate the effect of thickness distribution on power efficiency. Figure 9 shows the performance trends of simulated NACA foils (with a sharp trailing edge shape configuration) over the range of oscillating frequencies and Reynold's number of 1100. These results show that the effects of thickness variation on power efficiency are small. The maximum difference in the peak values of power efficiency occurs

at f^*=0.16 showing an overall variation of around 2%, whereas the peak efficiency value of 33.3% is at f^*=0.14 for NACA0015 sharp edge configuration.

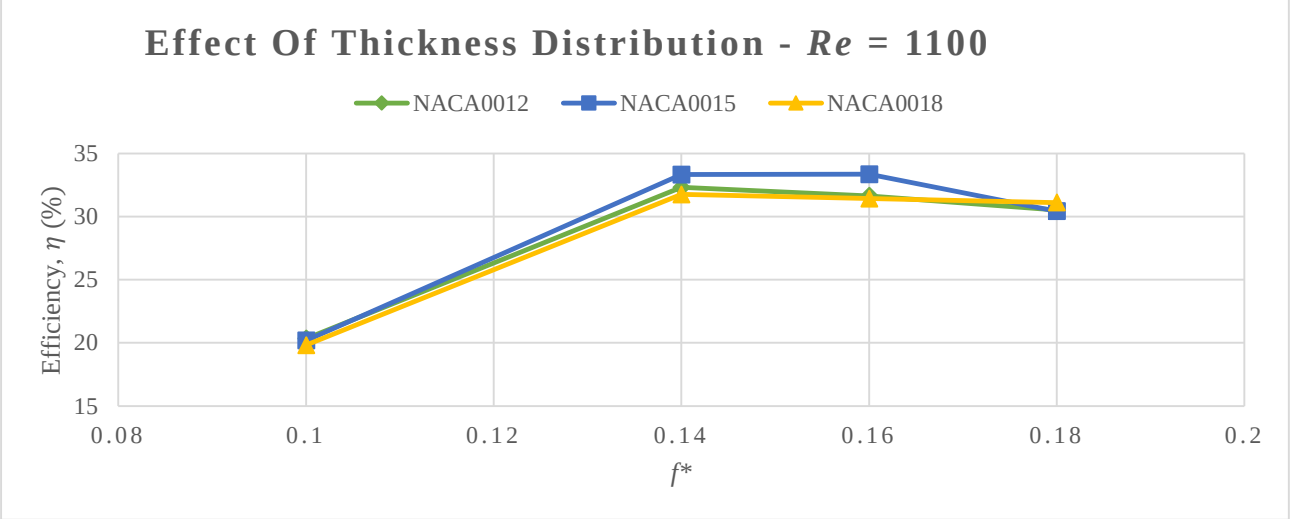

Figure 9: Comparison between NACA0012, NACA0015 and NACA0018 on power extraction efficiency in laminar flow field

Airfoil	Case 1 $f^* = 0.14$ Sharp edge		Case 2 $f^* = 0.16$ Blunt edge		Case 3 $f^* = 0.20$ Round edge	
	$\bar{C}_P$	η	$\bar{C}_P$	η	$\bar{C}_P$	η
NACA0012	0.82	32.3%	0.72	28.4%	0.60	23.6%
NACA0015	0.85	33.3%	0.71	27.7%	0.62	24.2%
NACA0018	0.80	31.4%	0.75	29.3%	0.57	22.2%

Table 4: Effect of airfoil thickness for selected trailing edge shape; *Re* = 1100

Further analysis on the effect of thickness distribution in laminar flow field has been carried by repeating the procedure at distinct trailing edge shapes. Selective iterations of simulated configurations have been compiled in Table 4. Case 2 demonstrates the effect of thickness variation on power performance subject to blunt edge truncation and oscillating frequency of 0.16. It highlights that the performance efficiency variation is of the similar magnitude, around 2%; similar to Case 1 and Case 3 featuring sharp and round edge truncations and operating at frequencies, f^* 0.14 and 0.20 respectively. Therefore it can be concluded that efficiency is mostly insensitive to the thickness distribution at low Reynold number (laminar flow field).

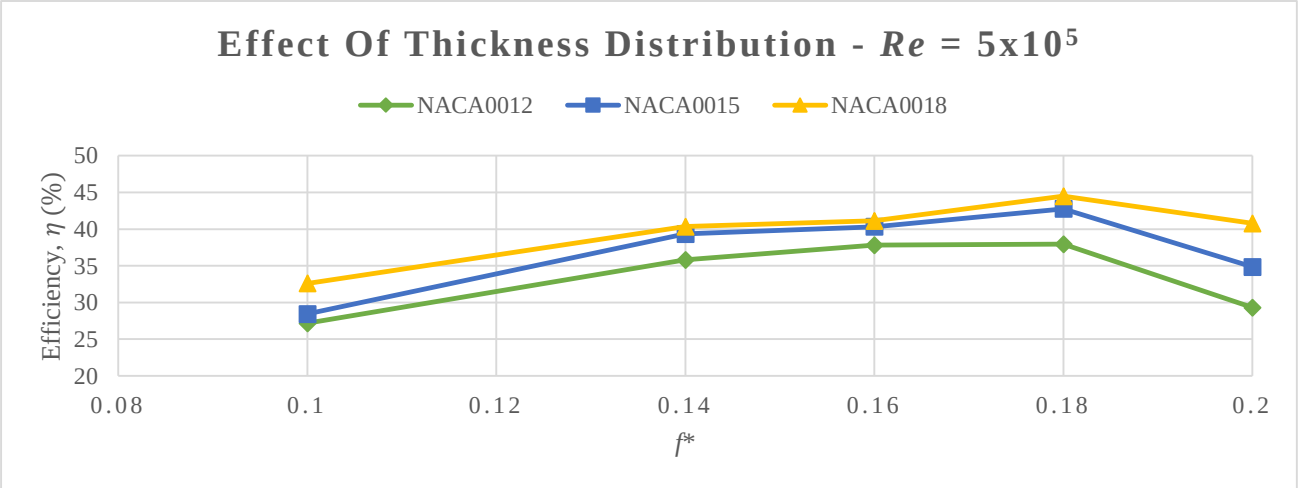

Figure 10: Comparison between NACA0012, NACA0015 and NACA0018 on power extraction efficiency in turbulent flow field

Subsequently the effect of thickness distribution at high Reynolds number has been investigated in this section. In standard trailing edge configuration the data presented in Figure 10 indicates the following trends: over the simulated range of frequencies the increase in thickness distribution results in higher power efficiency values. The thicker airfoil geometries steadily generate higher efficiency values as compared to the thinner foils, as it can be seen that NACA0018 shows a consistent higher efficiency values as compared to NACA0015 and likewise the NACA0015 as compared to NACA0012. The peak value of 44.49% for efficiency is obtained at $f^* = 0.18$ for the NACA0018, showing an increase of 6.5% as compared to NACA0012.

In the design space range of f^* it has been observed that the thinner airfoil geometries show higher gradients as compared to thicker airfoils before and after the peak efficiency values, as shown in Figure 10. The difference in performance efficiency continues to increase over the frequency range. It shows that at oscillating frequency, f^* = 0.16, 0.18 (peak efficiency value, Figure 10) and 0.20, the difference in performance efficiency is 2.5%, 6.5% and 11.5%, respectively between NACA0012 and NACA0018.

	Case 1		Case 2		Case 3	
	$f^* = 0.16$	Sharp edge	$f^* = 0.18$	Blunt edge	$f^* = 0.20$	Round edge
Airfoil	$\bar{C}_P$	η	$\bar{C}_P$	η	$\bar{C}_P$	η
Naca0012	0.96	37.8%	0.82	32.1%	0.46	18.2%
Naca0015	1.03	40.3%	0.90	35.2%	0.73	28.5%
Naca0018	1.05	41.1%	0.99	38.9%	0.89	34.8%

Table 5: Effect of airfoil thickness for selected trailing edge shape; *Re* = 5 x 10^5

Table 5 shows the effect of airfoil thicknesses for different trailing edge shapes and frequencies. From this table, it can be seen that there is about 16% efficiency difference between NACA0012 and NACA0018 by having a round trailing edge at frequency of 0.20. Moreover, it is found that the increase in thickness distribution in case of blunt and round trailing edge configurations has positive impact on the performance efficiency. Therefore it can be concluded that, at high Reynolds number (or in turbulent flow field) thickness distribution does have a positive impact on the power performance with the thicker airfoil.

B. Effect of Trailing Edge Shape on Performance Efficiency

In order to increase the yield of oscillating energy harvesting systems, optimum geometrical combination of thickness distribution and trailing edge shapes are searched in specific fluid flow conditions. Therefore in this section, following the conclusion from the above section (effect of thickness distribution on performance efficiency) that thicker airfoil has a more positive impact on the power performance at high Reynolds number, here NACA0015 and NACA0018 airfoils have been chosen for laminar and turbulent flows in order to further investigate over the design space range of frequencies and trailing edge configurations.

Figure 11 presents the effect of trailing edge modification on energy extraction characteristics of laminar flow, NACA0015 over range of oscillating frequencies. The peak efficiency value is achieved at frequency, $f^* = 0.14$. The data shown in Figure 11 highlights that sharp trailing configuration with peak efficiency value of 33.3% show approximately 7% higher values as compared to the least efficient blunt trailing edge configuration, which is approximately 26.4% efficiency. Similar performance behaviour is seen at higher off peak values. Therefore it can be concluded that the sharp trailing edge configuration is optimum for laminar flow field and NACA0015.

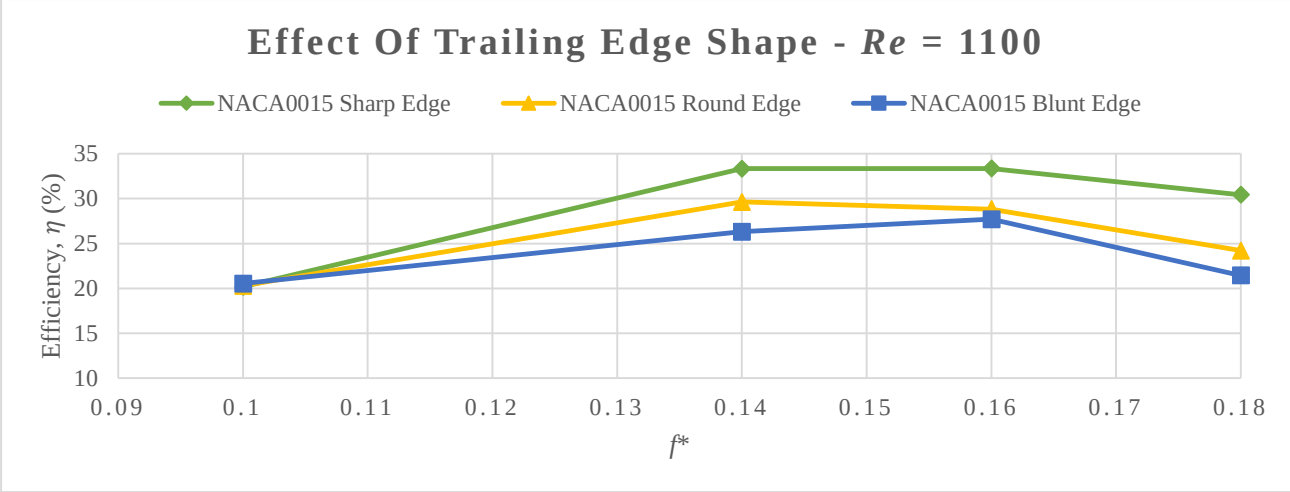

Figure 11: Comparison between sharp, round and blunt trailing edge shape for NACA0015

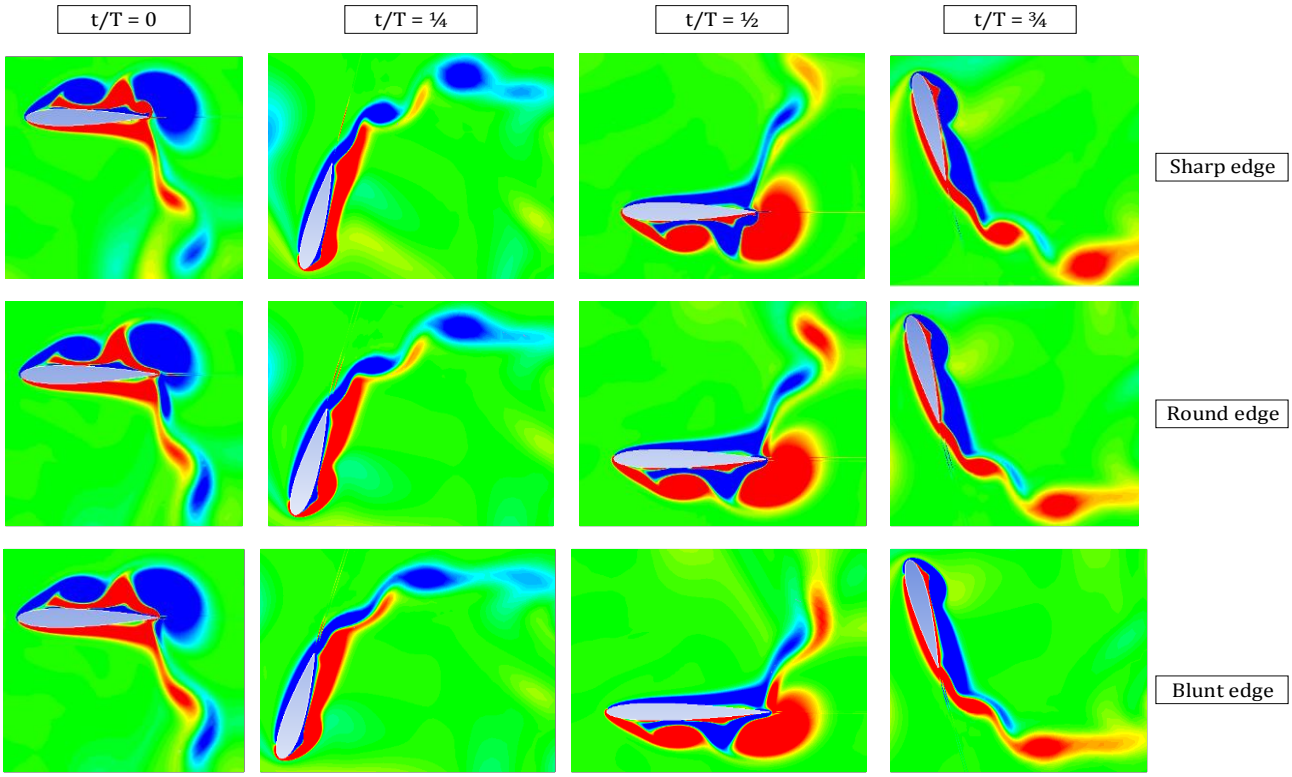

Figure 12: Vorticity fields (red: counter clockwise vorticity, blue: clockwise vorticity) for NACA0015, f^*= 0.14, *Re* =1100 at sharp, round and blunt trailing edge shape

Figure 12 shows the variation in vorticity strength between sharp, round and blunt edges. It can be seen that the vorticity influence is limited to the near wake and trailing edge region. This is due to the differences at the trailing edge shape which is less than 1% difference from the whole geometry.

For turbulence flow field analysis, the optimum airfoil geometry NACA0018 is further investigated for trailing edge shape variation and the power efficiency trends are shown in Figure 13. The sharp trailing edge shape still shows the best performance at each frequency tested. For all three trailing edge shapes that have been tested, the peak efficiency was reached at the oscillating frequency of 0.18. The corresponding peak efficiency values of approximately 44.5%, 38.9% and 37.7% are obtained for sharp, blunt and round trailing edge configurations, respectively.

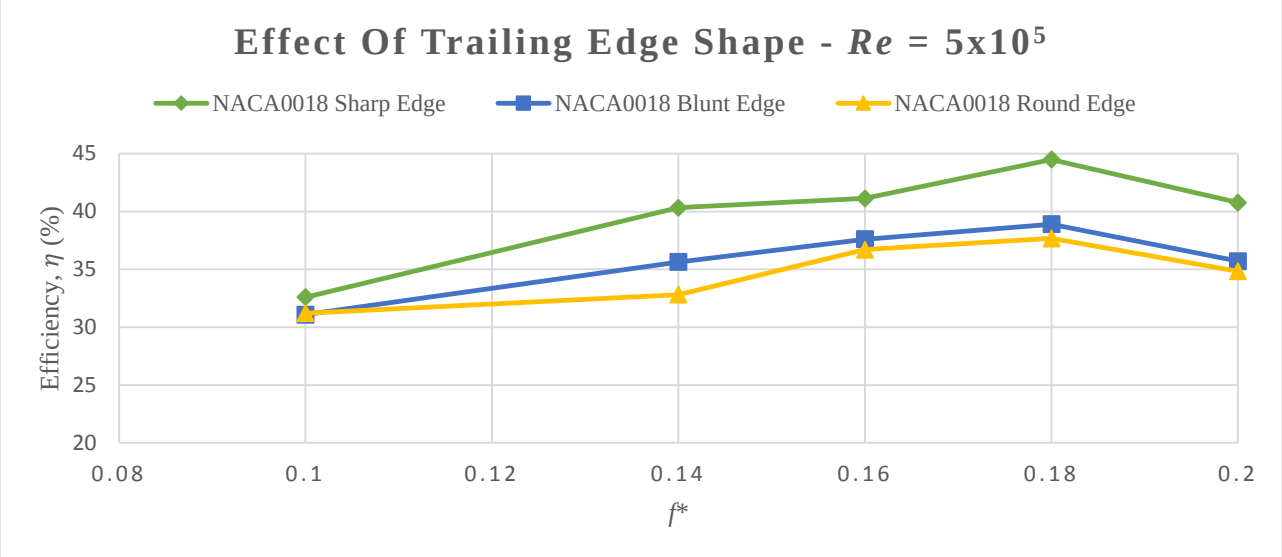

Figure 13: Comparison between sharp, round and blunt trailing edge shape for NACA0018

	NACA0012		NACA0015		NACA0018	
	$\bar{C}_P$	η	$\bar{C}_P$	η	$\bar{C}_P$	η
Sharp	0.9677	37.95%	1.0901	42.75%	1.1344	44.49%
Blunt	0.8195	32.14%	0.8987	35.24%	0.9918	38.90%
Round	0.7826	30.69%	0.8097	31.75%	0.9606	37.67%

Table 6: Parametric study of flows over different trailing edge shape and different thickness distribution

Table 6 shows a comparison of power efficiency and the mean power coefficient at various trailing edge shapes at the optimum frequency ($f^* = 0.18$), for NACA0012, NACA0015 and NACA0018. The data for NACA0012 and NACA0015 show a similar trend as in case of NACA0018. For NACA0012 and NACA0015, the sharp trailing edge shows the highest efficiency value followed by the blunt and round trailing edges, respectively. About 7% difference in power efficiency has been observed between sharp and round edges for NACA0012 and NACA0018 airfoils, while about 11% changes have occurred between sharp and round trailing edges for NACA0015.

Figure 14 shows the vorticity contour for the full cycle of NACA0018 having sharp trailing edge. It show the flow structure around the airfoil at frequency 0.18 for the whole cycle.

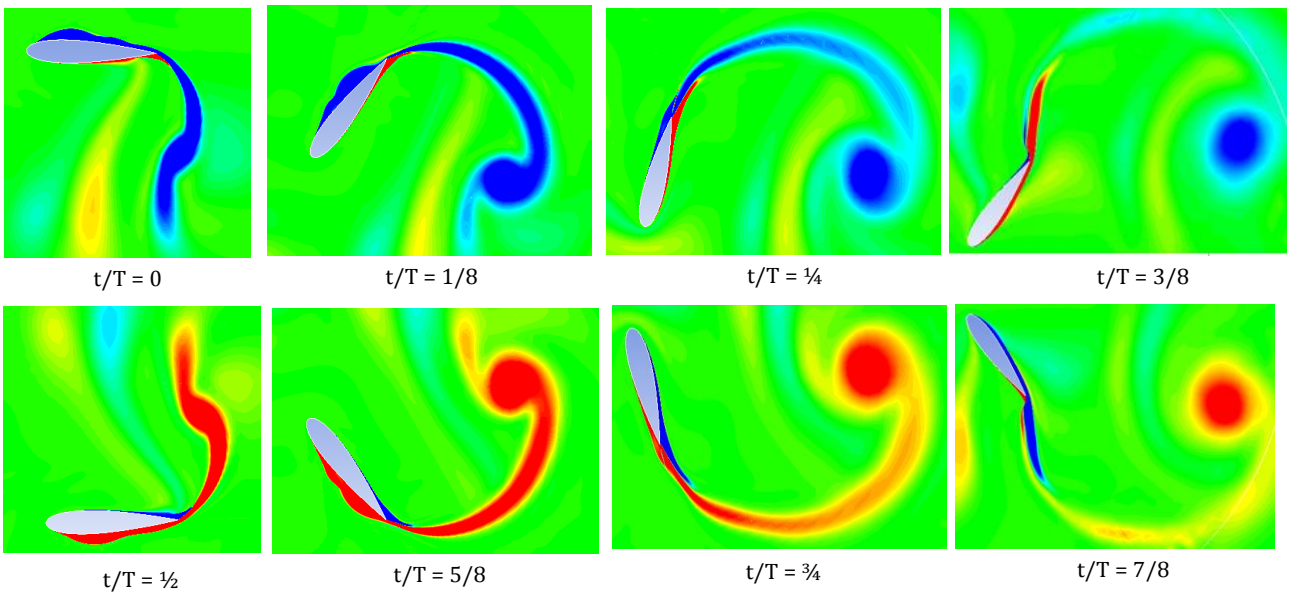

Figure 14: Vorticity fields (red: counter clockwise vorticity, blue: clockwise vorticity) for the entire cycle for NACA0018 having sharp trailing edge shape at Re = 5x10^5, f*=0.18.

Conclusion

In this study, numerical simulations of oscillating airfoils with different geometrical shapes have been carried for power extraction. Simulations have been run in laminar and turbulent flow field on symmetric NACA profile having different thicknesses distribution of 12%, 15% and 18%, and different trailing edge shapes variation (sharp, blunt and round edges). This study have been simulated at the range of frequency, $f^* = 0.10 - 0.20$, and at fixed heaving and pitching amplitudes, and has mainly focussed on the performance of power generation over the entire cycle.

It has been concluded that for the applied conditions of system shape and fluid kinematics, the effect of fluid physics at higher Reynolds numbers has shown higher efficiency values. Moreover, it has been observed that the geometry modifications have significant influence on the performance, and more specifically the trailing edge shape, as compared to thickness distribution. Under turbulent flow field, the results indicates that thickness distribution improves the efficiency performance by having a thick airfoil geometry. About 11.5% efficiency improvement has been observed between NACA0018 and NACA0012 at f* = 0.20. However, simulation at laminar flow does not show a significant difference when thickness is changed, which is found to be less than 2% difference over the range of tested frequency.

This study shows that the geometrical modification at the trailing edge shape does have an effect on the power efficiency. The sharp trailing edge configuration has indicated highest power efficiency values in both laminar and turbulent flow regimes, with 33.3% and 44.5%, respectively. Moreover, it has been found that the optimal power efficiency is achieved at comparatively low frequency value of $f^* = 0.14$ for laminar and $f^* = 0.18$ for turbulent flow.

Reference

[1] N. Armaroli and V. Balzani, “Towards an electricity-powered world,” pp. 3193–3222, 2011.

[2] M. O. Schiermeier Q., Tollefson Q., Scully T., Witze A., “Electricity without carbon,” *Nature*, vol. 454(7206), no. August, pp. 816–823, 2008.

[3] Q. Xiao, W. Liao, S. Yang, and Y. Peng, “How motion trajectory affects energy extraction performance of a biomimic energy generator with an oscillating foil ?,” *Renew. Energy*, vol. 37, no. 1, pp. 61–75, 2012.

[4] F. Pearce, “Current power: new tide turbines tab oceans of energy,” *New Sci.*, vol. 2830(Septe, pp. 48–51, 2011.

[5] J. Peng and G. S. Chen, “Flow-Oscillating Structure Interactions and the Applications to Propulsion and Energy Harvest,” *Appl. Phys. Res.*, vol. 4, no. 2, pp. 1–14, Apr. 2012.

[6] J. Young, J. C. S. Lai, and M. F. Platzer, “A review of progress and challenges in flapping foil power generation,” *Prog. Aerosp. Sci.*, vol. 67, pp. 2–28, May 2014.

[7] J. McKinney, W., DeLaurier, “The Wingmill: An Oscillating-Wing Windmill,” *J. Energy*, vol. 5.2, pp. 109–115, 1981.

[8] T. Kinsey and G. Dumas, “Parametric Study of an Oscillating Airfoil in a Power-Extraction Regime,” *AIAA J.*, vol. 46, no. 6, pp. 1318–1330, Jun. 2008.

[9] M. F. Young, J., Ashraf, M. A., Lai, J. C. S., Platzer, “Numerical simulation of flow-driven flapping-wing turbines for wind and water power generation,” in *17th Australasian fluid mechanics conference, Ackland, New Zealand*, 2010.

[10] W. Shyy and H. Liu, “Flapping Wings and Aerodynamic Lift: The Role of Leading-Edge Vortices,” *AIAA J.*, vol. 45, no. 12, pp. 2817–2819, 2007.

[11] M. a. Ashraf, J. Young, J. C. S. Lai, and M. F. Platzer, “Numerical Analysis of an Oscillating-Wing Wind and Hydropower Generator,” *AIAA J.*, vol. 49, no. 7, pp. 1374–1386, Jul. 2011.

[12] Q. Xiao and Q. Zhu, “A review on flow energy harvesters based on flapping foils,” *J. Fluids Struct.*, vol. 46, pp. 174–191, Apr. 2014.

[13] jones K. D. and P. M. F, “Numerical computation of flapping-wing propulsion and power extraction,” *AIAA J.*, 1997.

[14] Pointwise, “Pointwise User Manual,” 2011.

[15] T. Kinsey and G. Dumas, “Computational Fluid Dynamics Analysis of a Hydrokinetic Turbine Based on Oscillating Hydrofoils,” vol. 134, no. February 2012, pp. 1–16, 2015.